



## Numerical Study of Laminar Fluid Flow and Heat Transfer in the Entrance Region of a Circular Pipe

Dr. Adil Abbas Alwan Almoosawy

Professor

Dept. of Mechanical Eng.

University of Babylon

Sawsan Abdul Settari Owadh

Asst. lecturer

Dept. of Mechanical Eng.

University of Babylon

### Abstract :

This research represents a theoretical study which deals with the developing steady, laminar, Newtonian and incompressible fluid flow and heat transfer through circular tube. The effects of heat conduction, body force, free convection, heat generation and viscous dissipation within the fluid are neglected. A computer program was built by using Gaussian elimination method to perform the numerical marching technique solution with finite difference method for two cases of heating, constant wall temperature and constant wall heat flux boundary conditions for different values of Reynolds number (500, 1000, 2000) and Prandtl number (1, 2.5, 5).

This approach provides a picture of the variation of the velocity and temperature profiles through the tube. The computational algorithm is able to calculate all the hydrodynamic properties such as velocities and pressure drop. Also it is able to predict all the thermal properties such as the temperature, bulk temperature, and local Nusselt number. The velocity profile becomes fully developed at approximately  $\frac{Le}{2a} = 0.05 Re$ , and the temperature distribution becomes fully developed at approximately  $\frac{Le}{2a} = 0.05 Re \cdot Pr$ , as expected.

### Introduction

Heating and cooling of fluids flowing inside conduits are among the most important heat transfer processes in engineering. The design and analysis of heat exchangers require a knowledge of heat transfer coefficient between the wall of the conduit and the fluid flowing inside it. The sizes of boilers, economizers, superheaters, and preheaters depend largely on the heat transfer coefficient between the inner surface of the tubes and the fluid. Also, in the design of air-conditioning and refrigeration equipment, it is necessary to evaluate heat transfer coefficient for fluids flowing inside ducts.

In long ducts, where the entrance effects are not important, the flow is laminar when Reynolds number values approach 2300, in the range of Reynolds numbers between 2300 and 10,000, a transition from laminar to turbulent flow takes place, the flow in this regime is called transitional. At a Reynolds number 10,000, the flow becomes fully turbulent [1]. But when the conduit is short, in addition to Reynolds number and Prandtl number, several other factors such as entrance effects can influence heat transfer by forced convection in a duct. Therefore, when dealing with internal flows in short ducts, it is important to be cognizant of the extent of "the entry region", depending on whether the flow is laminar or turbulent.

A brief literature review indicates that Moller [2] presented Nusselt number data in laminar flow for conditions of either uniform wall temperature or uniform heat flux in fully-developed flow. Flow that was thermally-developing (where the heated section was preceded by an isothermal length exceeding the hydrodynamic entry length), and flow that was developing simultaneously both thermally and hydrodynamically, Al-Ali [3], a new integral method of solution for the combined

hydrodynamic and thermal-entrance-region problem for laminar flow through parallel-plate channels and circular tubes, was developed. The new analysis adapts the hydrodynamic inlet-filled region to the thermal entry length problem, Shirely and Joao [4], the generalized integral transform technique (GITT) was applied to the solution of the momentum equation in a hydrodynamically developing laminar flow of a non-Newtonian power-law fluid inside a circular ducts.

In this context, the present study applies the boundary layer model near the tube walls with a potential core toward the center of the tube which accelerates as the boundary layer grows. This model does an adequate job in most respects, it is questionable only near the tube inlet where transverse momentum effects are important and hence the boundary layer model breaks down.

## 2. Analytical model

Analytical model was presented for the partial differential equations which described the developing laminar fluid flow and heat transfer through circular tube, assuming incompressible and constant property flow for developing velocity and temperature profile through the circular tube. Figure.1 represents the viscous flow through pipe, and the coordinate system for the flow.

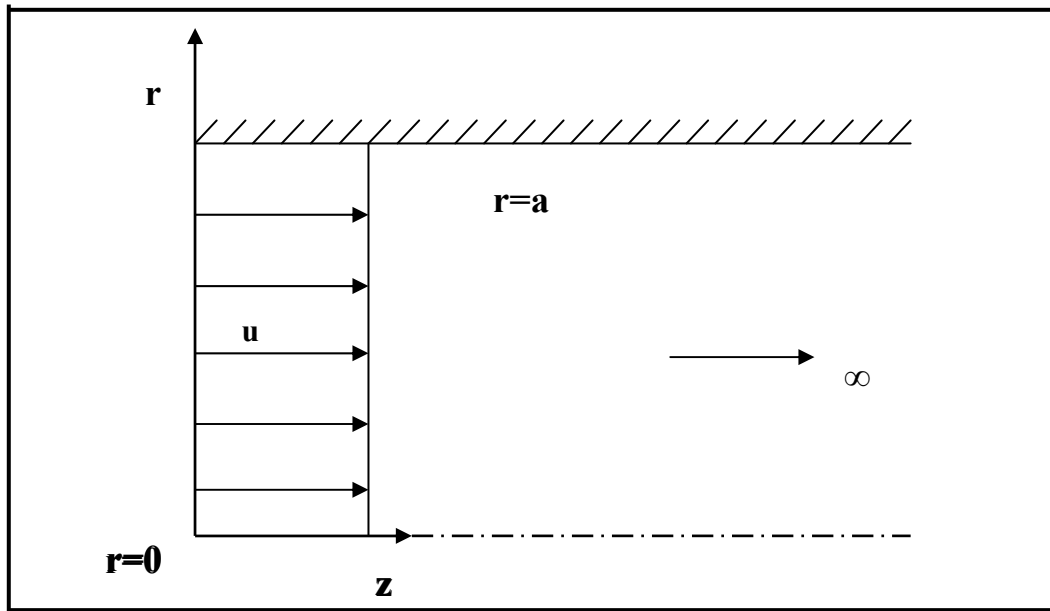


Figure 1: Schematic diagram of the problem

### Governing Equations

The boundary layer equations describing the present system are [5] :

#### Continuity equation

$$r \frac{\partial u}{\partial z} + \frac{\partial (v \cdot r)}{\partial r} = 0 \quad (1)$$

#### z-Momentum equation

$$u \frac{\partial u}{\partial z} + v \frac{\partial u}{\partial r} = -\frac{1}{\rho} \frac{dp}{dz} + \nu \left( \frac{\partial^2 u}{\partial r^2} + \frac{1}{r} \frac{\partial u}{\partial r} \right) \quad (2)$$

The energy equation for incompressible, constant property flow was uncoupled from the momentum equation once the velocity distribution was known. When viscous dissipation is neglected, the energy equation may be written as:

#### Energy equation

$$u \frac{\partial T}{\partial z} + v \frac{\partial T}{\partial r} = \alpha \left( \frac{\partial^2 T}{\partial r^2} + \frac{1}{r} \frac{\partial T}{\partial r} \right) \quad (3)$$

### Boundary Conditions

#### 1. Entrance Region Boundary Conditions

$$\left. \begin{aligned} u(r, 0) &= u_o \\ p(0) &= p_o \\ T(r, 0) &= T_o \end{aligned} \right\} \quad (4)$$

#### 2. Wall Boundary Conditions

$$\left. \begin{aligned} u(a, z) &= 0 \\ v(a, z) &= 0 \end{aligned} \right\} \quad (5)$$

$$T(a, z) = T_w \quad (\text{constant wall temperature}) \quad (6)$$

$$-k \frac{\partial T}{\partial r}(a, z) = q'' \quad (\text{constant wall heat flux}) \quad (7)$$

#### 3. Centerline of Tube Boundary Conditions

$$\left. \begin{aligned} \frac{\partial u}{\partial r}(0, z) &= 0 \\ v(0, z) &= 0 \\ \frac{\partial T}{\partial r}(0, z) &= 0 \end{aligned} \right\} \quad (8)$$

### Dimensionless Variables

$$\left. \begin{aligned} U &= \frac{u}{u_o} \\ V &= \frac{v}{u_o} \\ R &= \frac{r}{a} \\ Z &= \frac{z}{a} \\ P &= \frac{p_o - p}{\rho \cdot u_o^2} \end{aligned} \right\} \quad (9)$$

$$\theta = \frac{T - T_w}{T_o - T_w} \quad (\text{constant wall temperature}) \quad (10)$$

$$\theta = \frac{k}{q'' a} (T - T_o) \quad (\text{constant wall heat flux}) \quad (11)$$

Therefore, the governing equations may be put in dimensionless form as:

$$R \frac{\partial U}{\partial Z} + \frac{\partial (V \cdot R)}{\partial R} = 0 \quad (12)$$

$$U \frac{\partial U}{\partial Z} + V \frac{\partial U}{\partial R} = -\frac{\partial P}{\partial Z} + \frac{1}{\text{Re}} \left[ \frac{\partial^2 U}{\partial R^2} + \frac{1}{R} \frac{\partial U}{\partial R} \right] \quad (13)$$

$$U \frac{\partial \theta}{\partial Z} + V \frac{\partial \theta}{\partial R} = \frac{1}{\text{Pr} \cdot \text{Re}} \left[ \frac{\partial^2 \theta}{\partial R^2} + \frac{1}{R} \frac{\partial \theta}{\partial R} \right] \quad (14)$$

Also the Boundary Conditions may be in Dimensionless form as:

#### 1. Entrance Region Dimensionless Boundary Conditions

$$\left. \begin{aligned} U(R, 0) &= 1 \\ P(0) &= 0 \end{aligned} \right\} \quad (15)$$

$$\theta(R,0) = 1 \quad (\text{For constant wall temperature}) \quad (16)$$

$$\theta(R,0) = 0 \quad (\text{For constant wall heat flux}) \quad (17)$$

## 2. Wall Dimensionless Boundary Conditions

$$\left. \begin{aligned} U(1, Z) &= 0 \\ V(1, Z) &= 0 \end{aligned} \right\} \quad (18)$$

$$\theta(1, Z) = 0 \quad (\text{For constant wall temperature}) \quad (19)$$

$$\frac{\partial \theta}{\partial R}(1, Z) = 1 \quad (\text{For constant wall heat flux}) \quad (20)$$

## 3. Centerline of Tube Dimensionless Boundary Conditions

$$\left. \begin{aligned} \frac{\partial U}{\partial R}(0, Z) &= 0 \\ V(0, Z) &= 0 \\ \frac{\partial \theta}{\partial R}(0, Z) &= 0 \end{aligned} \right\} \quad (21)$$

## Heat Transfer Solution

### 1. Bulk Temperature

In order to solve for the heat transfer in confined flow situation, it is first necessary to find the bulk (mixed-mean) temperature. Ref.[5] is defined for the circular tube as :

$$T_b = \frac{\int_0^a 2 \pi r u T dr}{\int_0^a 2 \pi r u dr} \quad (22)$$

So equation (22) can be put in dimensionless form for both (CWT) and(CHF) cases as:

$$\theta_b = \frac{\int_0^1 2 \pi R U \theta dR}{\int_0^1 2 \pi R U dR} \quad (23)$$

where :

$$\theta_b = \frac{T_b - T_w}{T_o - T_w} \quad (\text{For constant wall temperature}) \quad (24)$$

$$\theta_b = \frac{k}{q'' a} (T_b - T_o) \quad (\text{For constant wall heat flux}) \quad (25)$$

$$\text{Where:} \quad \int_0^1 2 \pi R U dR = 1$$

### 2. Local Nusselt number

The local Nusselt number is given by Ref.[5] as:

$$Nu_z = \frac{2 h a}{k} \quad (26)$$

where

$$h(T_w - T_b) = k \left. \frac{\partial T}{\partial r} \right|_{r=a} \quad (27)$$

so

$$Nu_z = \frac{-\left. \frac{\partial T}{\partial r} \right|_{r=a}}{T_b - T_w} \cdot (2a) \quad (28)$$

**So, the dimensionless local Nusselt Number for constant wall temperature:**

$$Nu_z = \frac{-2 \left. \frac{\partial \theta}{\partial R} \right|_{R=1}}{\theta_b} \quad (29)$$

**And, the dimensionless local Nusselt Number for constant heat flux :**

$$Nu_z = \frac{-2}{\theta_b - \theta_w} \quad (30)$$

### 3. Numerical Techniques

The above equations were solved using the marching technique with finite difference method as presented by Horenbeck [5]. A grid is now imposed on the new field as shown in figure 2,

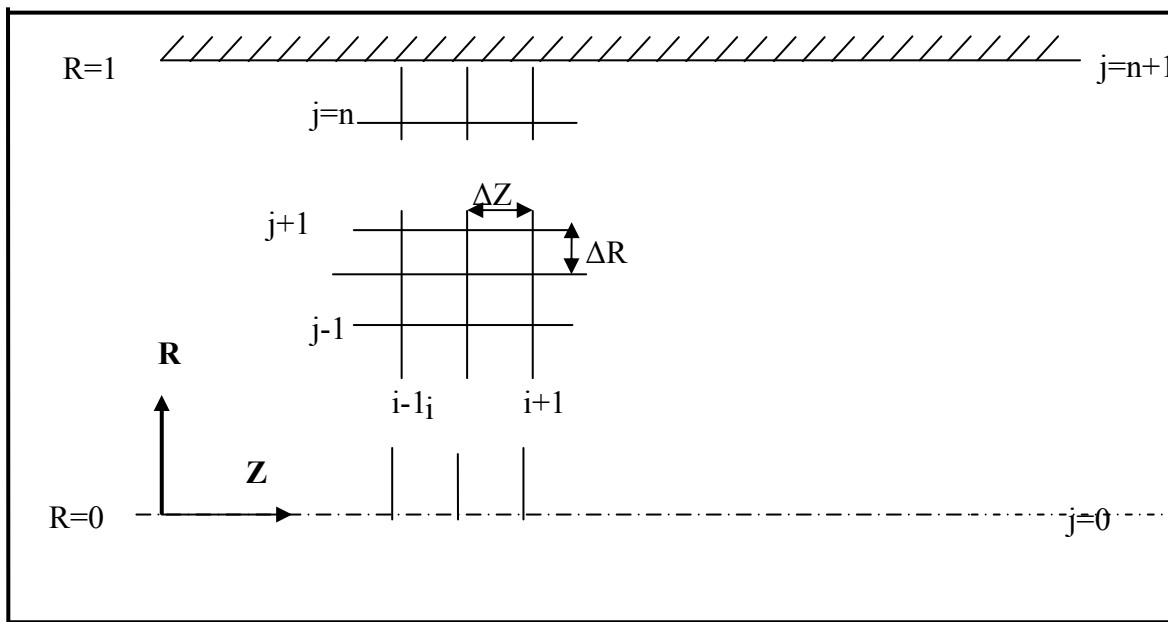


Figure 2: Finite difference representation to be used with basic equations.

And the representations used for these equations at an interior node  $(i,j)$  are :

$$U_{i,j} \frac{U_{i+1,j} - U_{i,j}}{\Delta Z} + V_{i,j} \frac{U_{i+1,j+1} - U_{i+1,j-1}}{2(\Delta R)} = -\frac{P_{i+1} - P_i}{\Delta Z} + \frac{1}{\text{Re}} \left[ \frac{U_{i+1,j+1} - 2U_{i+1,j} + U_{i+1,j-1}}{(\Delta R)^2} + \frac{1}{R_j} \frac{U_{i+1,j+1} - U_{i+1,j-1}}{2(\Delta R)} \right] \quad (31)$$

Equation (31) represents numerical formulation for the dimensionless form of z-momentum equation, And Horenbec [5] showed that the numerical formulation of continuity equation is :

$$\left[ \frac{R_j (U_{i+1,j} - U_{i,j})}{2(\Delta Z)} + \frac{R_{j+1} (U_{i+1,j+1} - U_{i,j+1})}{2(\Delta Z)} \right] + \frac{V_{i+1,j+1} R_{j+1} - V_{i+1,j} R_j}{\Delta R} = 0 \quad (32)$$

these equations may be written at  $R=0$  as :

$$U_{i,0} \frac{U_{i+1,0} - U_{i,0}}{\Delta Z} = - \frac{P_{i+1} - P_i}{\Delta Z} + 4 \left[ \frac{U_{i+1,1} - U_{i+1,0}}{(\Delta R)^2} \right] \quad (33)$$

$$\frac{U_{i+1,1} + U_{i+1,0} - U_{i,1} - U_{i,0}}{2(\Delta Z)} + \frac{2V_{i+1,1}}{\Delta R} = 0 \quad (34)$$

Equations (31) and (32) are written for  $j=1(1)n$  and equations (33) and (34) for  $j=0$  together constitute  $(2n+2)$  equations in the  $(2n+2)$  unknowns  $(U_{i+1,j}, V_{i+1,j})$ ; and  $(P_{i+1})$ .

The system of equations may be considerably reduced in size by using the integral continuity equation . Adding the continuity equation (32) for  $J=1(1)n$  and equation (33) for  $J=0$  together , the resulting equation can be written in the form :

$$\Delta R \left( \frac{1}{4} U_{i+1,0} + \frac{3}{4} U_{i+1,1} \right) + \sum_{j=2}^n R_j U_{i+1,j} = \Delta R \left( \frac{1}{4} U_{i,0} + \frac{3}{4} U_{i,1} \right) + \sum_{j=2}^n R_j U_{i,j} \quad (35)$$

It is now convenient to rewrite equation (31) as:

$$\left[ -\frac{V_{i,j}}{2(\Delta R)} - \frac{1}{2 \text{Re} \cdot R_j (\Delta R)} - \frac{1}{\text{Re} (\Delta R)^2} \right] U_{i+1,j-1} + \left[ \frac{U_{i,j}}{\Delta Z} + \frac{2}{\text{Re} (\Delta R)^2} \right] U_{i+1,j} \\ + \left[ \frac{V_{i,j}}{2(\Delta R)} - \frac{1}{2 \text{Re} \cdot R_j (\Delta R)} - \frac{1}{\text{Re} (\Delta R)^2} \right] U_{i+1,j+1} + \frac{1}{\Delta Z} P_{i+1} = \frac{U_{i,j}^2 + P_i}{\Delta Z} \quad (36)$$

And equation (33) as:

$$\left[ \frac{U_{i,0}}{\Delta Z} + \frac{4}{\text{Re} (\Delta R)^2} \right] U_{i+1,0} - \left[ \frac{4}{\text{Re} (\Delta R)^2} \right] U_{i+1,1} + \left( \frac{1}{\Delta Z} \right) P_{i+1} = \frac{U_{i,0}^2 + P_i}{\Delta Z} \quad (37)$$

Equation (36) written for  $J=1(1)n$  , equation (37) for  $J=0$  ,and equation (35) now comprise  $(n+2)$  linear algebraic equations in the  $(n+2)$  unknowns  $U_{i+1,j}$  and  $P_{i+1}$ . This set of equations may be written in matrix form, the matrix of coefficients does not have the desirable tridiagonal character of the matrices. This matrix is, however, quite sparse. It would be possible to write a special computer program by taking full advantage of this sparseness. This would only be practical if a large number of production runs were contemplated and the savings in running time and storage space considered more important than the programming time required. As a general rule, it seems most practical to solve the set by using one of the standard routines for linear equations or matrix inversion which are available at any computer installation. A possible alternative is to solve the set by Gaussian elimination method. This method will work effectively except for equation (35) [top row of this matrix which must be drastically under relaxed.

After the set has been solved for  $(U_{i+1,0}, \dots, U_{i+1,n})$  and  $(P_{i+1})$ , equation (32) may be employed in the form:

$$V_{i+1,j+1} = \left( \frac{R_j}{R_{j+1}} \right) V_{i+1,j} - \frac{\Delta R}{2(\Delta Z)} \left[ U_{i+1,j+1} - U_{i,j+1} + \left( \frac{R_j}{R_{j+1}} \right) (U_{i+1,j} - U_{i,j}) \right] \quad (38)$$

which may be marched outward from the tube centerline to give the values of  $(V_{i+1,1}, \dots, V_{i+1,n})$ .

Another step  $(\Delta Z)$  downstream may now be taken and the process repeated. This may be continued as many times until reach to  $(0.001)$  percentage error of iteration.

The proper choice of the  $(\Delta Z)$  mesh size at and near the tube entrance is a very important factor in obtaining an accurate solution. The entrance itself represents a mathematical difficulty in that it behaves like a singularity. This mathematical singularity may be dealt with in the manner described for the leading edge in the boundary layer development problem, by keeping  $(\Delta Z)$  very

small and hence taking a large number of steps in the region close to the entrance. As in the boundary layer case, the spread of the effect of the singularity downstream is primarily a function of how many steps are taken to reach a given (Z) position. If a large number of steps are taken to reach this value of (Z), then the effect of the singularity there tends to disappear. The effect of the singularity may thus be confined to a region arbitrarily close to the entrance.

### Finite Difference Representation for Dimensionless Energy Equation

Equation (14) may now be expressed in an implicit finite difference form similar to that used for the momentum equation in the preceding section. This difference form is :

$$U_{i,j} \frac{\theta_{i+1,j} - \theta_{i,j}}{\Delta Z} + V_{i,j} \frac{\theta_{i+1,j+1} - \theta_{i+1,j-1}}{2(\Delta R)} = \frac{1}{\text{Pr} \cdot \text{Re}} \left[ \frac{\theta_{i+1,j+1} - 2\theta_{i+1,j} + \theta_{i+1,j-1}}{(\Delta R)^2} + \frac{1}{R_j} \frac{\theta_{i+1,j+1} - \theta_{i+1,j-1}}{2(\Delta R)} \right] \quad (39)$$

This equation applies for  $j=1(1)n$

For  $R=0$  it is again necessary to apply the limiting process as  $(R \rightarrow 0)$  to equation (39), which results in

$$U \left. \frac{\partial \theta}{\partial Z} \right|_{R=0} = \frac{2}{\text{Re} \cdot \text{Pr}} \left( \left. \frac{\partial^2 \theta}{\partial R^2} \right) \right|_{R=0} \quad (40)$$

Expressing equation (40) in finite difference form yields :

$$U_{i,0} \left[ \frac{\theta_{i+1,0} - \theta_{i,0}}{\Delta Z} \right] = \frac{4}{\text{Re} \cdot \text{Pr}} \left[ \frac{\theta_{i+1,1} - \theta_{i+1,0}}{(\Delta R)^2} \right] \quad (41)$$

Equation (41) includes the symmetry condition expressed as:

$$\theta_{i+1,1} = \theta_{i+1,-1} \quad \text{at } R=0$$

Equation (39) and (41) may be rewritten in more useful forms as:

$$\left[ \frac{-V_{i,j}}{2(\Delta R)} + \frac{1}{2 \text{Re} \cdot \text{Pr} \cdot R_j (\Delta R)} - \frac{1}{\text{Re} \cdot \text{Pr} (\Delta R)^2} \right] \theta_{i+1,j-1} + \left[ \frac{U_{i,j}}{\Delta Z} + \frac{2}{\text{Re} \cdot \text{Pr} (\Delta R)^2} \right] \theta_{i+1,j} + \left[ \frac{V_{i,j}}{2(\Delta R)} - \frac{1}{2 \text{Re} \cdot \text{Pr} \cdot R_j (\Delta R)} - \frac{1}{\text{Re} \cdot \text{Pr} (\Delta R)^2} \right] \theta_{i+1,j+1} = \frac{U_{i,j} \cdot \theta_{i,j}}{\Delta Z} \quad (42)$$

And

$$\left[ \frac{U_{i,0}}{\Delta Z} + \frac{4}{\text{Re} \cdot \text{Pr} (\Delta R)^2} \right] \theta_{i+1,0} + \left[ \frac{-4}{\text{Re} \cdot \text{Pr} (\Delta R)^2} \right] \theta_{i+1,1} = \frac{U_{i,0} \cdot \theta_{i,0}}{\Delta Z} \quad (43)$$

If the wall temperature is constant, equation (42) written for  $j=1(1)n$  and equation (43) for  $j=0$  constitute a set of  $(n+1)$  linear algebraic equations in the  $(n+1)$  unknowns  $\theta_{i+1,j}$ . This set may be written in matrix form, this matrix equation is tridiagonal and the method illustrated in (Ref.[5]) is used to obtain a solution for the  $(\theta_{i+1,j})$ 's.

For the constant heat flux case, the wall temperature  $(\theta_{i+1,n+1})$  becomes an additional unknown. the necessary additional equation is supplied by the wall heat flux condition in (20) expressed in finite difference form as :

$$\frac{3\theta_{i+1,n+1} - 4\theta_{i+1,n} + \theta_{i+1,n-1}}{2(\Delta R)} = 1 \quad (44)$$

By using the backward difference in (Ref.[5]). This additional equation must now be added to the previous system of equations and the complete set may be written in matrix form which has a tridiagonal matrix of coefficients and the method of (Ref.[5]) is used.

After the solution has been obtained another step downstream may be taken and the process is repeated . It is of course best to obtain the velocity and temperature solutions together, solving first at each step for the velocity and then for the temperature .

## Heat Transfer Solution

### 1. Dimensionless Bulk Temperature ( $\theta_b$ )

The dimensionless bulk temperature ( $\theta_b$ ) is calculated numerically by employing Simpson's rule:

$$\theta_b \big|_{i+1} = \frac{\Delta R}{3} \left( 4 \sum_{j=1,3,5,7,\dots}^n U_{i+1,j} R_j \theta_{i+1,j} + 2 \sum_{j=2,4,6,8,\dots}^{n-1} U_{i+1,j} R_j \theta_{i+1,j} \right) \quad (45)$$

### 2. Local Nusselt Number ( $Nu_z$ )

The Nusselt number is given by equation (28). The local Nusselt number for constant wall temperature boundary condition is given by equation (29), which is written in a finite difference form as,

$$N_{uz} = -2 \frac{(3\theta_{i+1,n+1} - 4\theta_{i+1,n} + \theta_{i+1,n-1})}{2(\Delta R)\theta_b \big|_{i+1}} \quad (46)$$

And the local Nusselt number for constant heat flux boundary condition is given by equation (30), which is written in a finite difference form as,

$$N_{uz} = \frac{-2}{\theta_b \big|_{i+1} - \theta_w \big|_{i+1}} \quad (47)$$

## 4. Results and Discussion

### A. Computational results for Hydrodynamics Parameters.

#### Dimensionless Velocity Profile Development

Figure (3) shows the dimensionless velocity profiles which represent the developing stages of the hydrodynamic boundary layer for different Reynolds numbers at the entrance region of the circular tube. Assuming uniform velocity ( $U=U_0=1$ ) over its inlet section. The dimensionless velocity at the walls equals zero, because of adhesion, and increases as moving towards the center at which the maximum value is existed.

Figure (4) shows the dimensionless velocity profiles in the developing and fully developed region for the three values of Reynolds numbers . In developing region ,for each value of Reynolds number the dimensionless velocity at the wall equals zero and increases with moving far away from the wall until it reaches a maximum value at the centerline of the tube. The maximum velocity increases with decreasing Reynolds number but the velocity near the wall increases with increasing Reynolds number. In other hand it can be seen that the relative boundary layer thickness decreases with increasing Reynolds number ,this is due to decreasing of friction factor.

In the fully developed region the velocity at the wall equals zero and increases gradually until it reach a maximum value at the centerline of the tube. The dimensionless velocity profile in the fully developed region is the same for each value of Reynolds number ,i.e. the velocity profiles in the fully developed region is independent of Reynolds number.

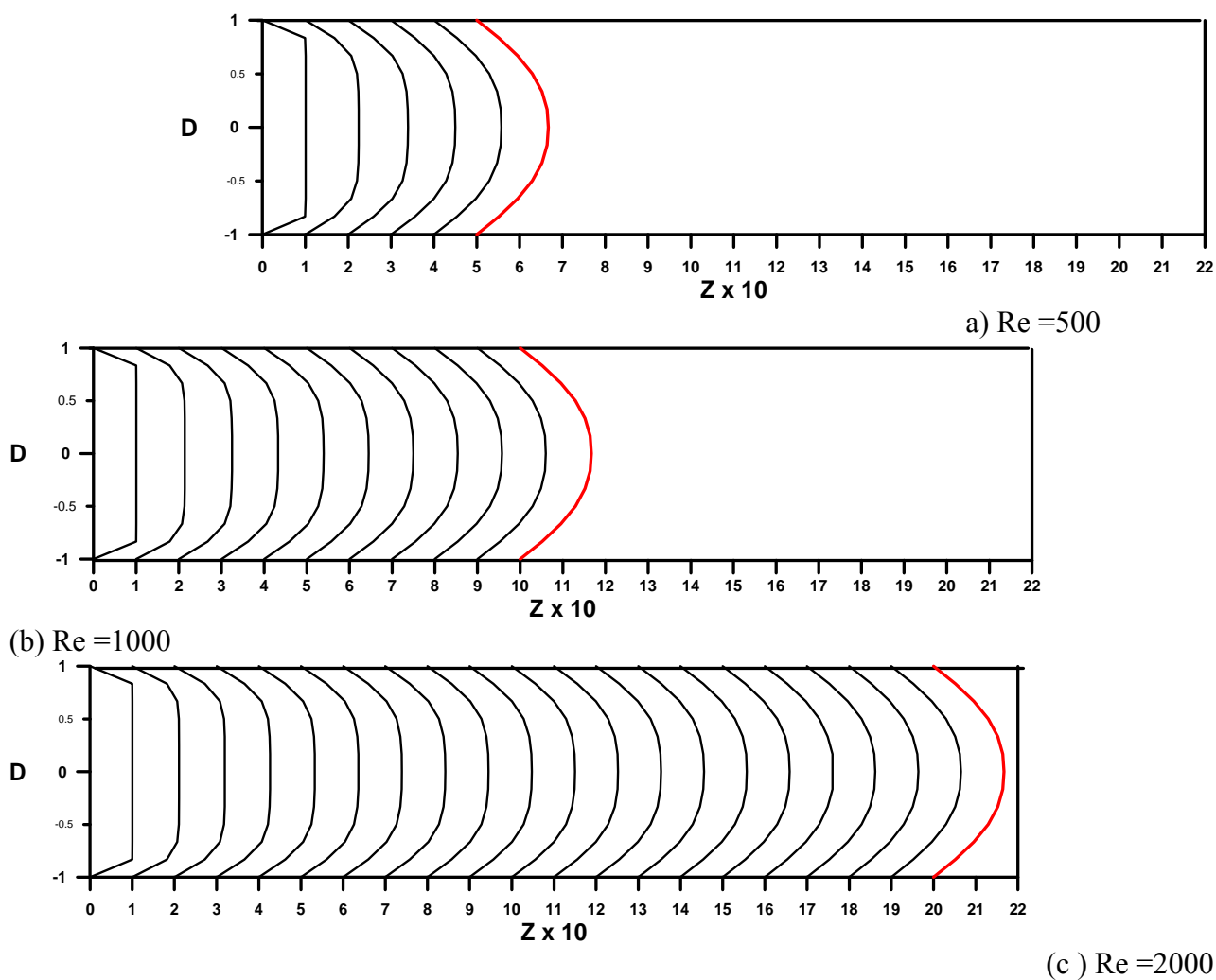
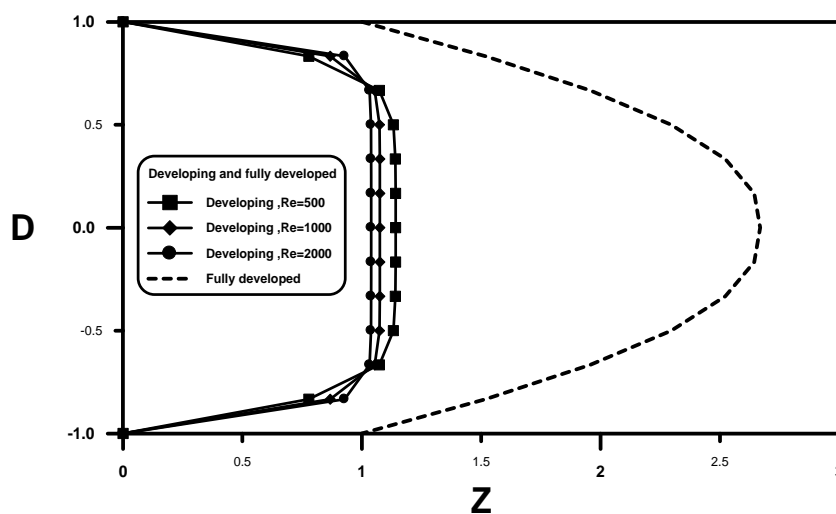


Figure 3: Hydrodynamic dimensionless velocity profile development through circular tube for different Reynolds numbers.



## B. Computational results for Thermal Parameters

### Dimensionless Temperature Distribution

#### A- At Constant Wall Temperature ( $\theta = \frac{T - T_w}{T_o - T_w}$ )

Figure(5) and figure (6) show the dimensionless temperature distribution for constant wall temperature boundary condition. These were manifested stages of developing of the thermal boundary layer for different Reynolds numbers ( $Re=500$ ) and ( $Re=2000$ ), and for different Prandtl numbers ( $Pr=1$ ), ( $Pr=2.5$ ) and ( $Pr=5$ ) at the entrance region of the circular tube.

The dimensionless temperature in the inlet section is uniformly distributed over its section and that its magnitude is ( $\theta=\theta_o=1$ ). The dimensionless temperature at the walls equals zero where ( $T=T_w$ ) but increases as moving far away from the tube surface, until it approaches the maximum value at the centerline of the tube. In each figure it can be noted that the thermal boundary layer approaches to the fully developed region faster as Prandtl number decreasing. In other hand, if we compare these figures, it can be noted that the thermal boundary layer approaches faster to the fully developed region as decreasing of Reynolds number, this is due to increasing of friction factor which leads to decreasing of mean velocity ( $u$ ). So, it can be concluded that the shape of the thermal boundary layer will be fixed after a certain distance from the entrance, which is called the thermal entry length ( $L_{et}$ ). It was noted that the thermal entrance length increases with increasing of Reynolds and Prandtl numbers. The temperature distribution becomes fully developed at approximately:

$$\frac{L_{et}}{2a} = 0.05 Re \cdot Pr$$

In the fully developed region the gradient of the dimensionless temperature  $\left( \frac{\partial \theta}{\partial Z} = 0 \right)$ , this is because the value of fluid temperature reaches to the value of the wall temperature.

Figures (7) and figure (8) show the developing and fully developed dimensionless temperature distribution through circular tube for constant wall temperature boundary condition and different Prandtl numbers. In developing region the dimensionless temperature at the walls equals zero where ( $T=T_w$ ) and increases as moving far away from the tube surface until it reach its maximum value at the centerline of the tube. The maximum dimensionless temperature increases with increasing Prandtl number. The dimensionless temperature near the wall increases with increasing Prandtl and Reynolds numbers. Each value of Reynolds and Prandtl numbers have the same dimensionless temperature distribution in fully developed region because the thermal boundary layer reach to its final form at this region where the fluid temperature reaches to a value equal approximately to the value of the wall temperature. So the temperature distribution in fully developed region is independent of Reynolds and Prandtl numbers.

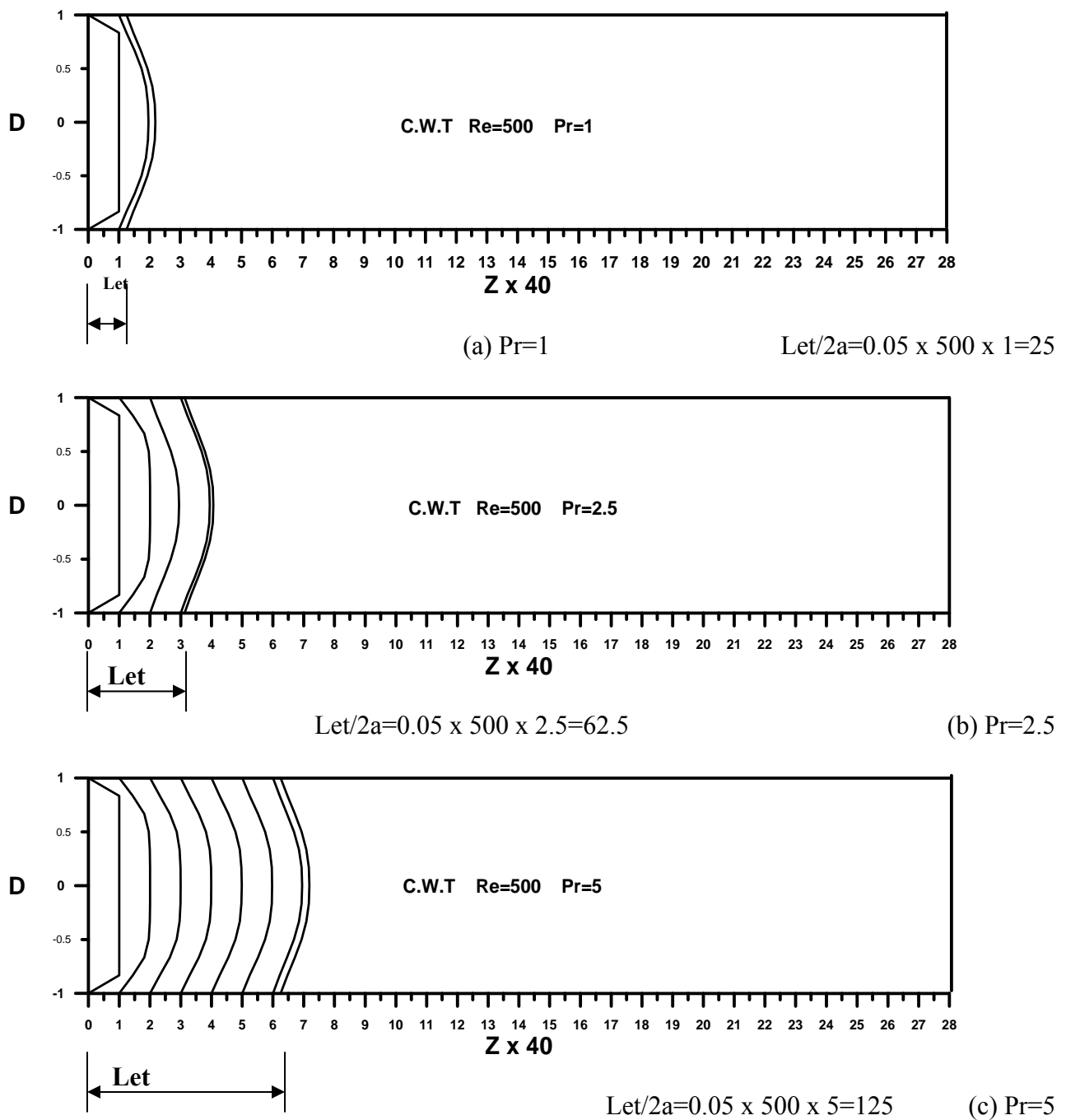


Figure 5: Dimensionless thermal temperature distribution development through circular tube for constant wall temperature,  $Re=500$ , different Prandtl number.

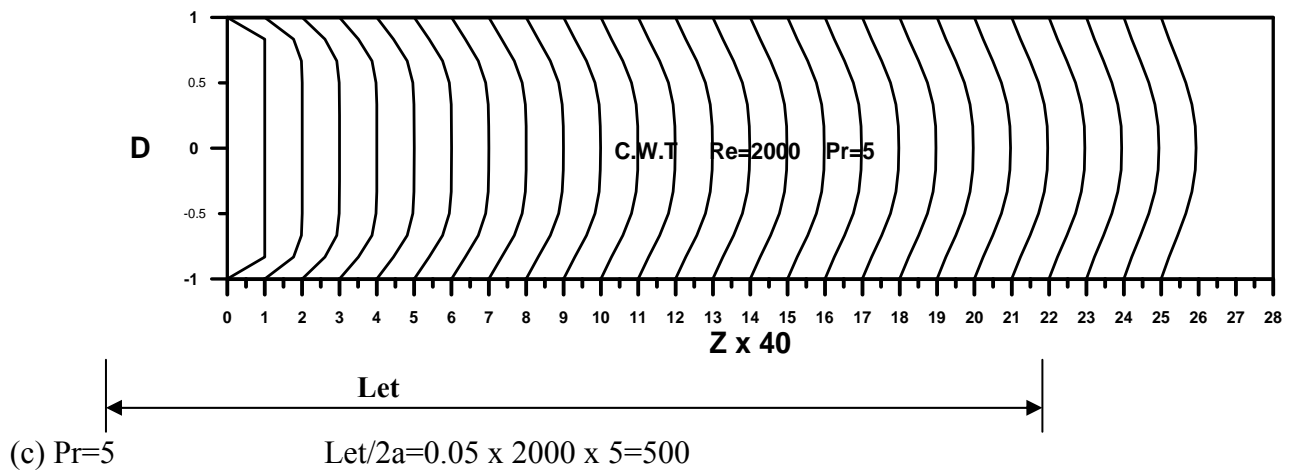
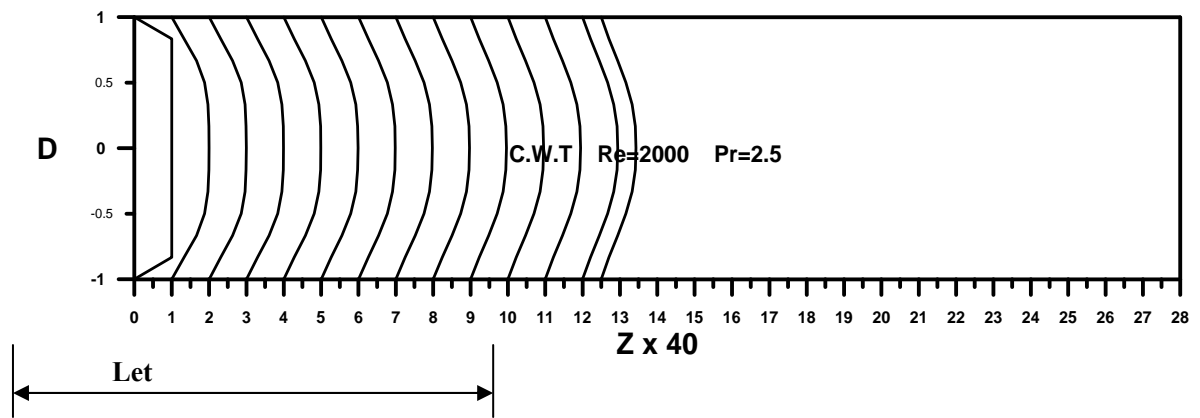
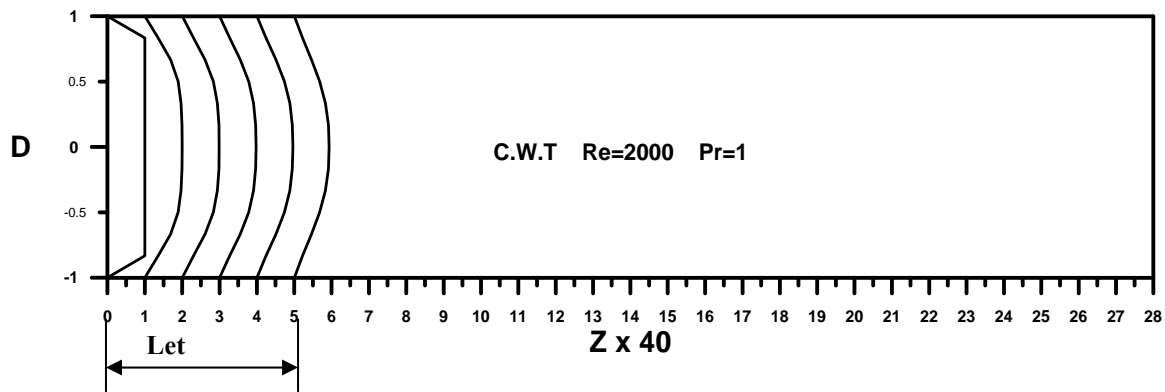


Figure 6: Dimensionless thermal temperature distribution development through circular tube for constant wall temperature , $Re=2000$ , different Prandtl number

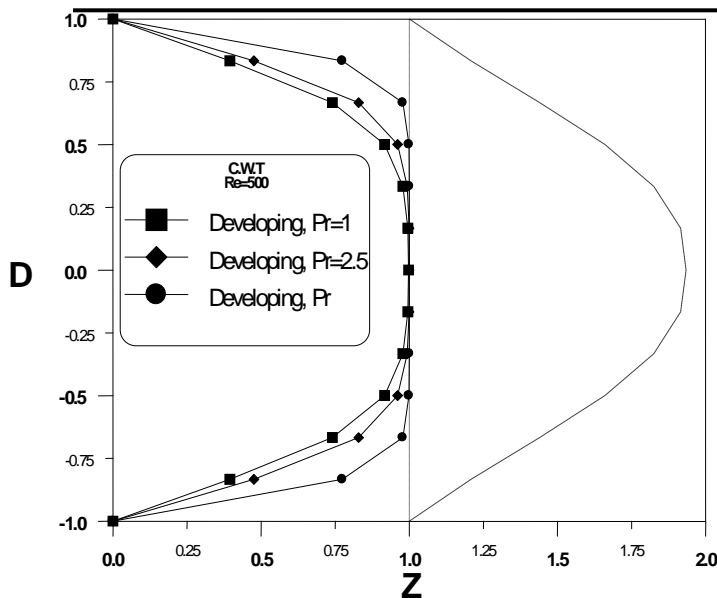


Figure 7: Developing and fully developed dimensionless temperature distribution through circular tube for constant wall temperature ,Re=500,

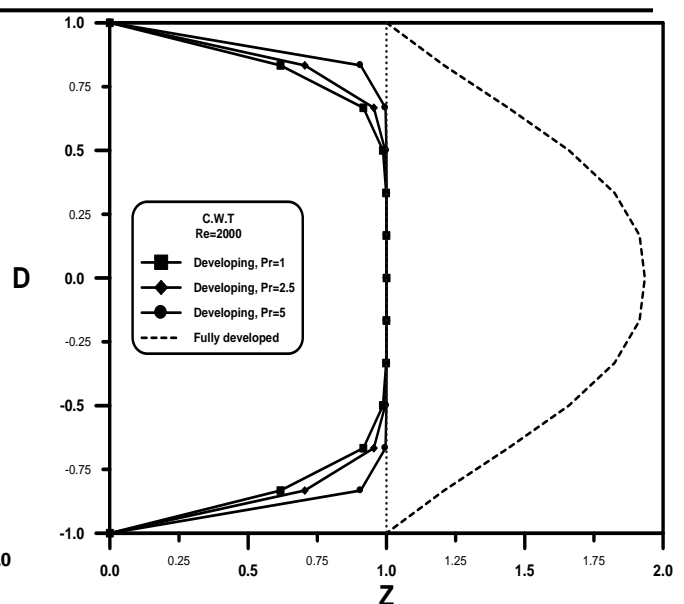


Figure 8: Developing and fully developed dimensionless temperature distribution through circular tube for constant wall temperature ,Re=2000,

### B – At Constant Heat Flux ( $\theta = \frac{T - T_o}{q'' a}$ )

Figure (9) and figure (10) show the dimensionless temperature distribution for constant heat flux boundary condition. These were manifest stages of developing of the thermal boundary layer for different Reynolds numbers (Re=500) and (Re=2000), and for different Prandtl numbers (Pr=1), (Pr=2.5) and (Pr=5) at the entrance region of the circular tube. The dimensionless temperature at the inlet section is zero over its section where ( $T=T_o$ ). The dimensionless temperature at the walls equals maximum value due to the effect of heat flux but decreases gradually with moving far away from the surface until it approaches minimum value at the centerline of tube. Where  $Pr = \frac{\nu}{\alpha}$  = kinematics viscosity / thermal diffusivity , so as ( $\alpha$ ) increase , Prandtl number will decrease , so the temperature profile will reach to the fully develop region faster . The shape of the thermal boundary layer will be fixed after a certain distance from the entrance. This distance is called the thermal entry length ( $Le_t$ ). It was noted that the thermal entrance length increases with increasing of Reynolds and Prandtl numbers. It can be seen that the thermal boundary layer is developed faster for lower Reynolds and Prandtl numbers. The temperature distribution becomes fully developed at approximately :

$$\frac{Le_t}{2a} = 0.05 Re . Pr$$

In the fully developed region the gradient of the dimensionless temperature ( $\frac{\partial \theta}{\partial Z} = 0$ ) , because the fluid temperature reaches to a value close to the wall temperature. However the flow field is similar for all studied cases.

Figure (11) and figure (12) show the developing and fully developed dimensionless temperature distribution through circular tube for constant heat flux boundary condition. These figures are for different Prandtl numbers (Pr=1), (Pr=2.5) and (Pr=5). In developing region the dimensionless temperature at the walls equals maximum value due to the effect of heat flux and decreases with moving far away from the surface until it approaches minimum value at the centerline of the tube. For developing region the change of dimensionless temperature usually occurs near the wall. In the fully developed region the dimensionless temperature start maximum

value at the wall and decreases until the minimum value of dimensionless temperature at the centerline of the tube. In the fully developed region all figures have same dimensionless temperature distribution because the thermal boundary layer reach to its final form at this region where the fluid temperature reaches to a value equal approximately to the value of the wall temperature . So the dimensionless temperature distribution in fully developed region is independent of Reynolds and Prandtl numbers

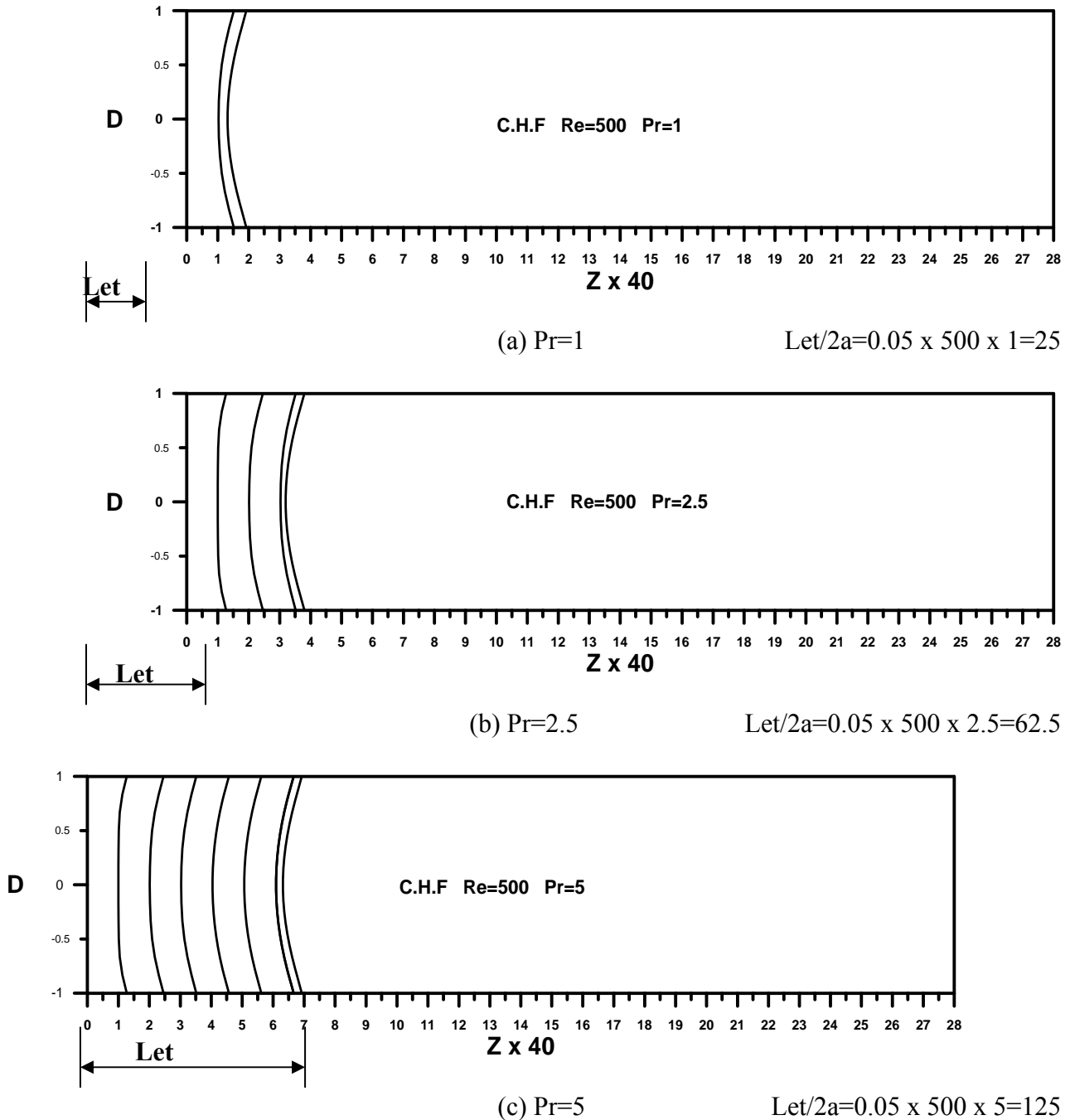
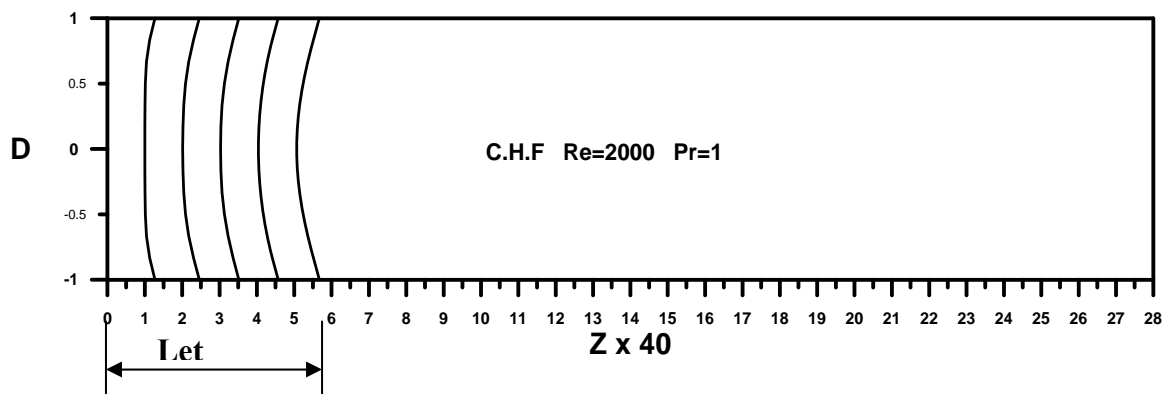
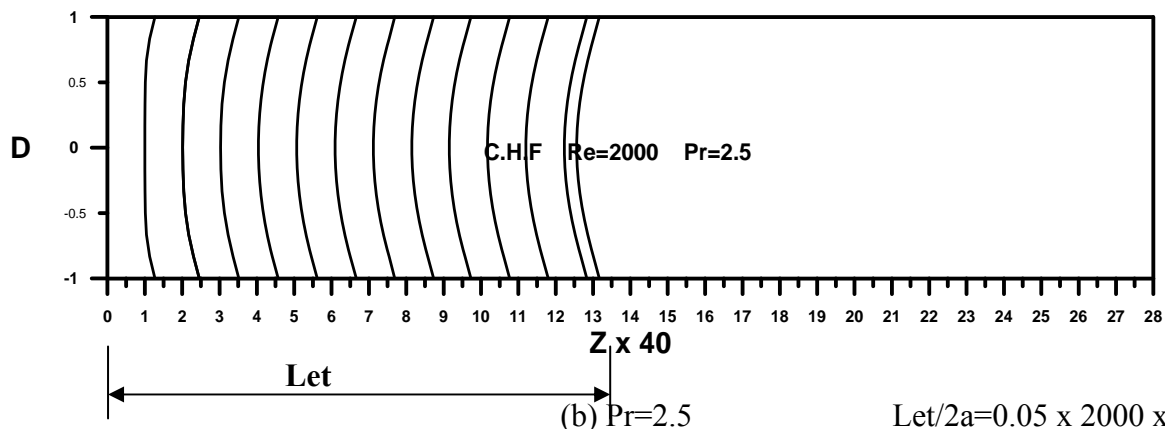


Figure 9 : Thermal temperature distribution development through circular tube  
for constant heat flux , $Re=500$  ,  
different Prandtl number



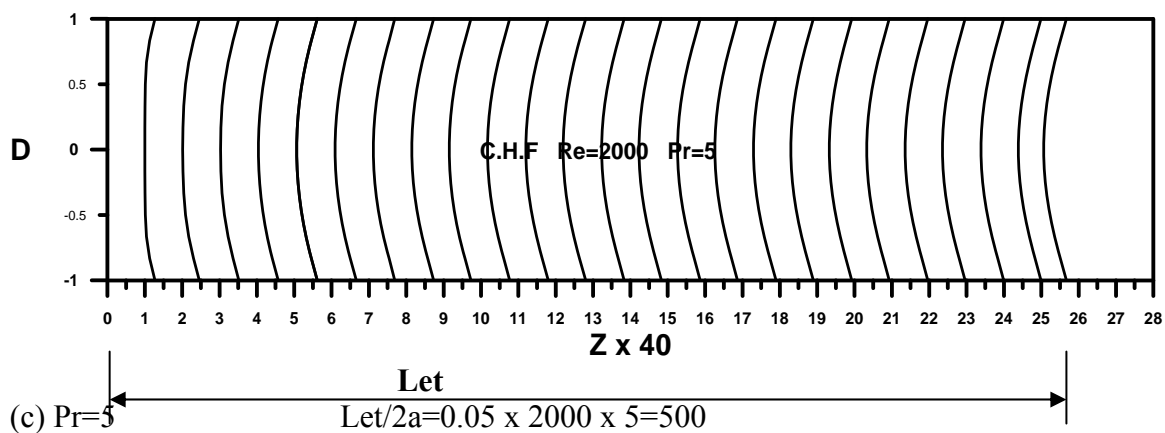
(a) Pr=1

$$Let/2a = 0.05 \times 2000 \times 1 = 100$$



(b) Pr=2.5

$$Let/2a = 0.05 \times 2000 \times 2.5 = 250$$



(c) Pr=5

$$Let/2a = 0.05 \times 2000 \times 5 = 500$$

Figure 10: Thermal temperature distribution development through circular tube for constant heat flux,  $Re=2000$ , different Prandtl number.

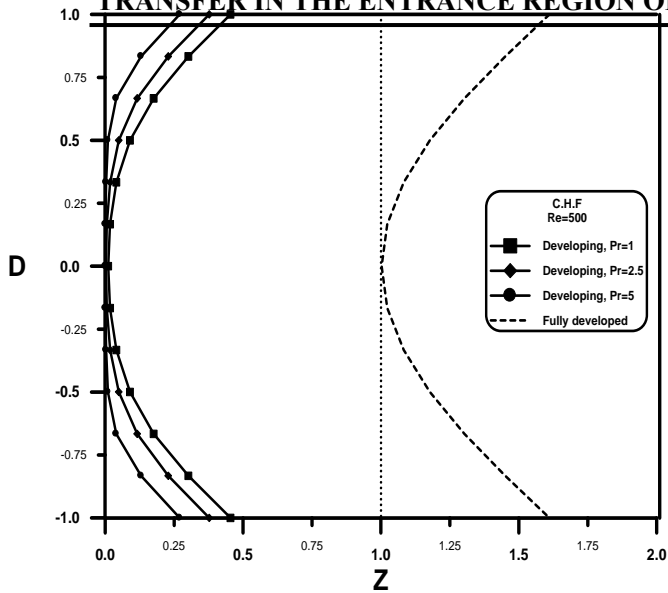


Figure 11: Developing and fully developed dimensionless temperature distribution through circular tube for constant heat flux ,  $Re=500$  , different Prandtl number

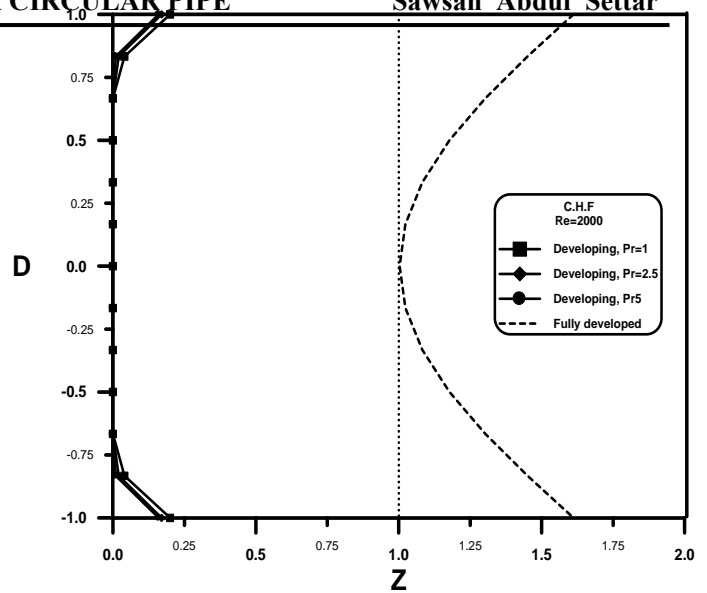


Figure 12: Developing and fully developed dimensionless temperature distribution through circular tube for constant heat flux ,  $Re=2000$  , different Prandtl number

### Dimensionless Bulk Temperature ( $\theta_b$ )

Figures 13 , 14 and figure 15, 16 show the dimensionless bulk temperature in developing region for Constant Wall Temperature and Constant Heat Flux boundary conditions respectively . For (CWT) boundary conditions ,at the inlet section of the tube where ( $T = T_o$ ) the dimensionless bulk temperature have a maximum value of one, and this value decreases with increasing the axial distance from inlet. For low Prandtl number the dimensionless bulk temperature is faster reach to the minimum value (approximately 0.1) . For (CHF) boundary conditions ,at the inlet section of the tube where( $T = T_o$ ) the dimensionless bulk temperature have a minimum value equals to zero and increases with increasing axial distance from inlet and reaches maximum value of approximately (0.92) at the thermally fully developed region. It can be concluded that the dimensionless bulk temperature depends on Prandtl, Reynolds number and the dimensionless axial distance ( $Z$ ).

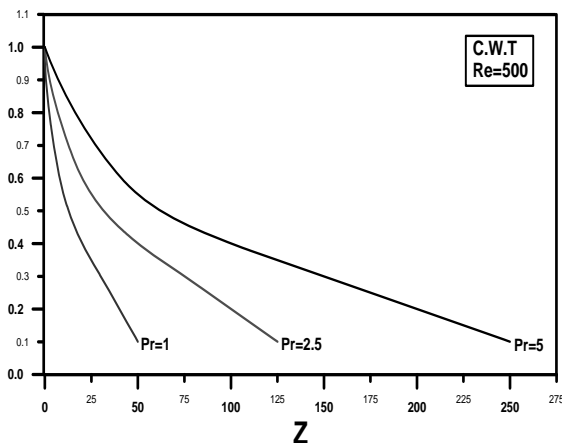


Figure 13: Dimensionless bulk temperature through circular tube for constant wall temperature ,  $Re=500$

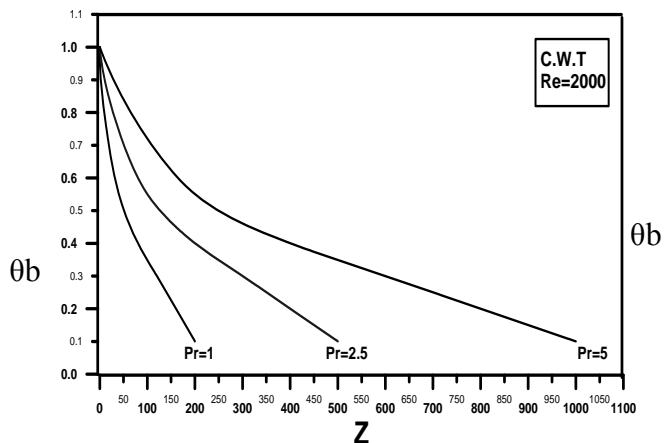


Figure 14: Dimensionless bulk temperature through circular tube for constant wall temperature ,  $Re=2000$

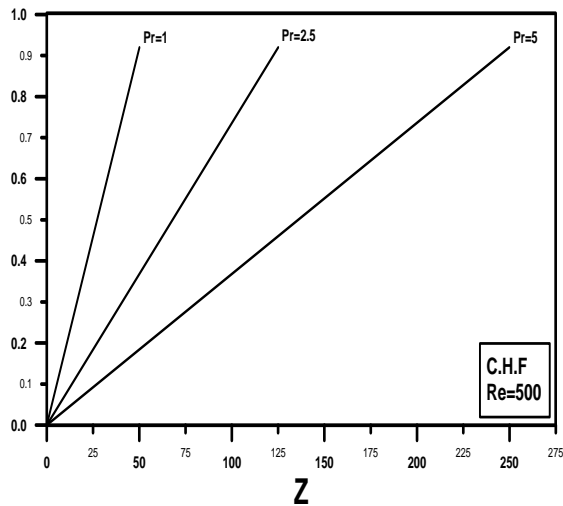


Figure 15: Dimensionless bulk temperature through circular tube for constant heat flux,  $Re=500$

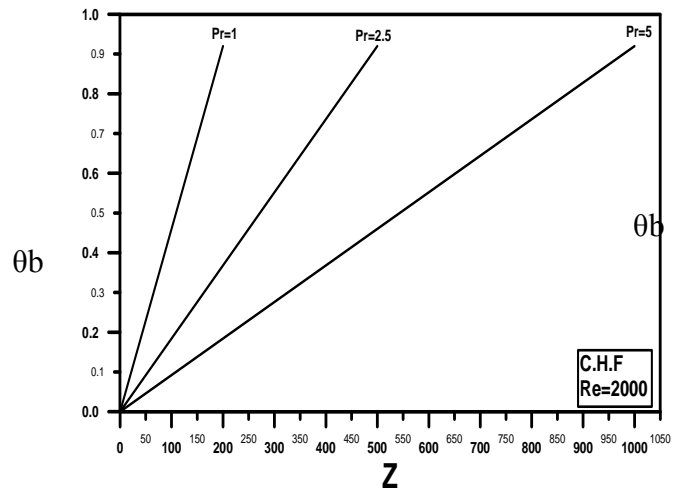


Figure 16: Dimensionless bulk temperature through circular tube for constant heat flux,  $Re=2000$

### Local Nusselt Number

Figures 17, 18 and figures 19, 20 show the axial development of local Nusselt number at the entrance region of circular tube with Reynolds numbers ( $Re=500$ ), ( $Re=1000$ ) and ( $Re=2000$ ) and different Prandtl numbers for Constant Wall Temperature and Constant Heat Flux boundary conditions respectively. For (CWT) boundary conditions, Nusselt number has a maximum value at the start of entrance region of approximately (12.2) and then decreases gradually until it has a minimum value of approximately (4.23) where it close to the thermal fully developed region. For (CHF) boundary condition, the maximum Nusselt number is (14.8), but the minimum value of Nusselt number is (4.3) for all Reynolds and Prandtl numbers.

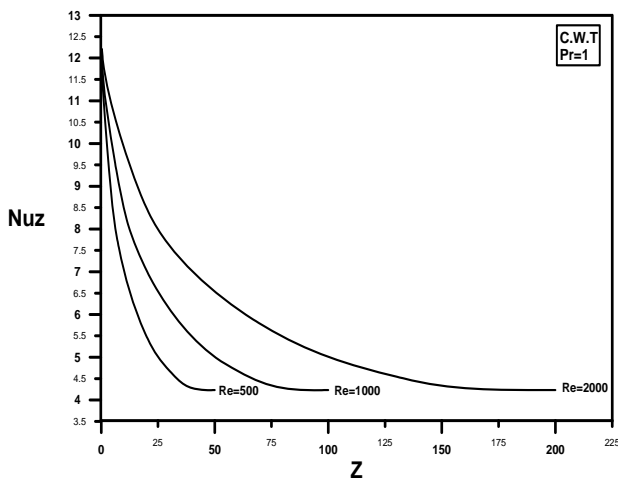


Figure 17: Local Nusselt number through circular tube for constant wall temperature,  $Pr=1$

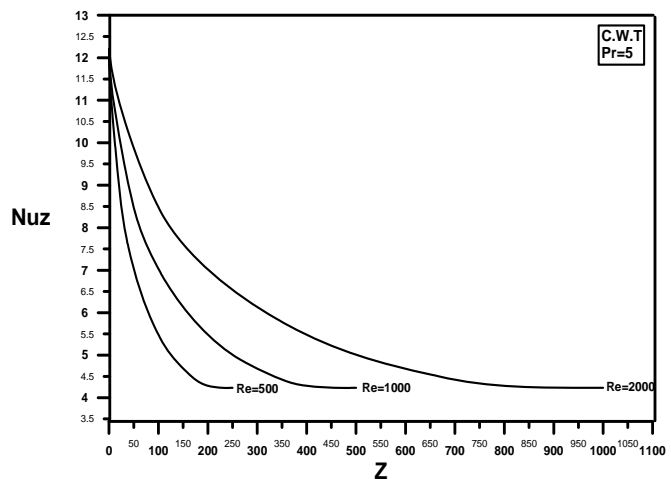


Figure 18: Local Nusselt number through circular tube for constant wall temperature,  $Pr=5$

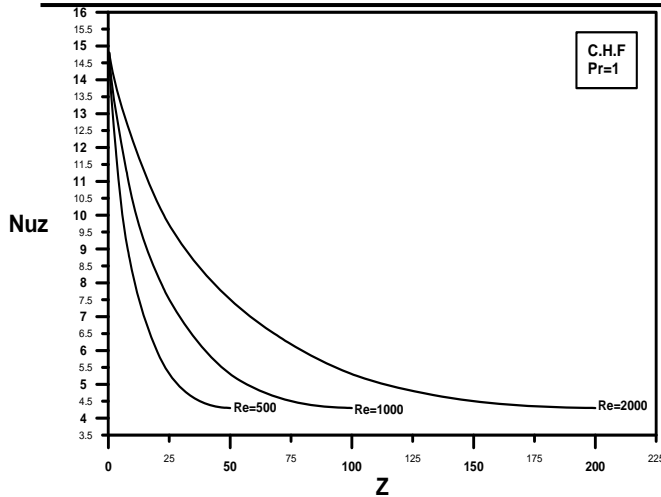


Figure 19: Local Nusselt number through circular tube for constant heat flux,  $Pr=1$

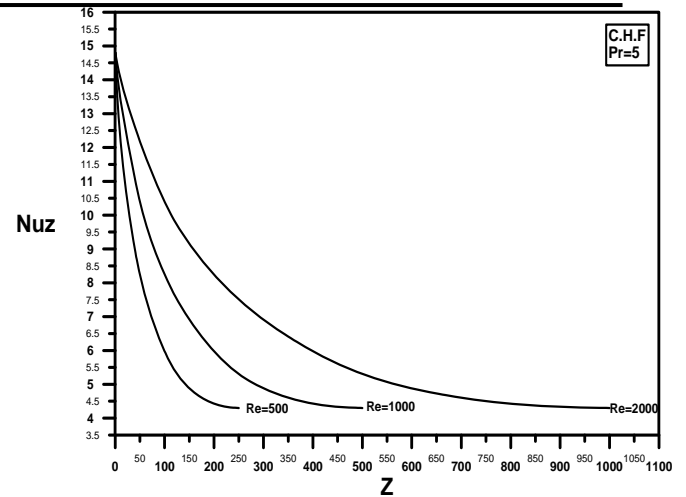


Figure 20: Local Nusselt number through circular tube for constant heat flux,  $Pr=5$

The boundary layer thickness is zero at the start of entrance region, hence, there is no resistance against heat transfer which leads to raise the heat transfer coefficient value to maximum. So the heat transfer coefficient decreases as the boundary layer begins the process of developing until it reaches a constant value. For low Reynolds and Prandtl numbers the local Nusselt number reaches faster the minimum value (small thermal entry length  $\frac{L_{et}}{2a} = 0.05 Re \cdot Pr$ ). It is noted that the local Nusselt number for the constant heat flux case is greater than the local Nusselt number for constant wall temperature case. A comparison of local Nusselt number of the present work for both cases of heating with a previous work is shown in table (1) below.

Reference	Local Nusselt number ( $Nu_z$ )			
	Constant wall temperature		Constant heat flux	
	maximum	minimum	maximum	minimum
Holman [6]	12.8	3.6	14.6	4.364
Present work	12.2	4.23	14.8	4.3

Also table (2) shows the convergence behavior of the dimensionless central axial velocity between the present work (numerical solution) and Ref.[4] which used the (GITT) analytically to solve the problem. These data are shown in figure (21), there is ( $\mp 0.03$ ) percentage error between

Z	Present work	Shirly and Joao
0.0005	1.1	1.08
0.00105	1.127	1.155
0.00125	1.233	1.166
0.005	1.41	1.363
0.012	1.61	1.607
0.0125	1.661	1.612
0.013	1.661	1.612
0.014	1.668	1.618

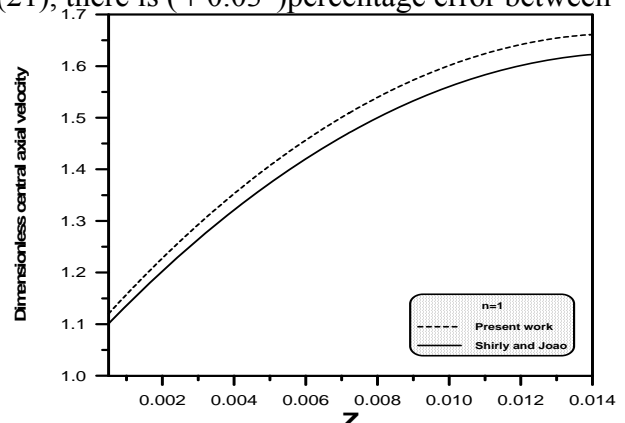


Figure 21: Convergence behavior of the dimensionless central axial velocity between the present work and Ref. [4]

## Conclusions

1. It can be seen that the boundary layer developed faster for lower Reynolds number. The maximum velocity is at the centerline of the tube. The velocity profile becomes fully developed at approximately ( $\frac{L_e}{2a} = 0.05 Re$ ) for laminar flow.

2. The maximum dimensionless temperature for constant wall temperature is at the centerline of the tube but for constant wall heat flux boundary condition is at the walls.
3. The thermal boundary layer developed faster for lower Reynolds and Prandtl numbers. The dimensionless temperature distribution becomes fully developed at approximately  $(\frac{L_{et}}{2a} = 0.05 \text{ Re} \cdot \text{Pr})$ .
4. The effect of the fluid flow features on the heat transfer behavior appears clearly in calculating bulk temperature, where the bulk temperature decreases in the developing region for constant wall temperature boundary condition, and the bulk temperature increases linearly in developing region for constant heat flux boundary condition. The bulk temperature decreases for constant wall temperature and increases for constant heat flux until its slope becomes zero. The zero slope of bulk temperature means that there is no heat transfer ( $\Delta T \approx 0$ ), because the fluid temperature was reached to a value close to the wall temperature.
5. The Nusselt number has the maximum value at the start of entrance region and then decreases gradually until it will be close to thermal fully developed region. This is due to the higher velocity at the inlet of the tube as comparing with that when moving far away in the axial direction from the inlet of the tube.
6. The Nusselt number at constant heat flux boundary condition is greater than Nusselt number at constant wall temperature boundary condition. However, the flow field is similar for all studied cases.

### **Nomenclature**

#### **Latin Symbols**

$a$  = The radius of circular tube  
 $d$  = Diameter of circular tube  
 $D$  = Dimensionless diameter of circular tube  
 $h$  = Heat transfer coefficient  
 $k$  = Thermal conductivity  
 $T$  = Temperature  
 $T_b$  = Bulk temperature  
 $\theta$  = Dimensionless temperature  
 $\theta_b$  = Dimensionless bulk temperature  
 $u$  = Velocity in axial direction  
 $U$  = Dimensionless velocity in axial direction  
 $v$  = Velocity in vertical direction

$L$  = Length of tube  
 $L_e$  = Hydrodynamic entry length  
 $L_{et}$  = Thermal entry length  
 $P$  = Pressure  
 $P$  = Dimensionless pressure  
 $q$  = Heat flux

$V$  = Dimensionless velocity in vertical direction  
 $Z$  = Dimensionless axial direction of the tube  
 $R$  = Dimensionless vertical direction of the tube

#### **Greek Symbols**

$\rho$  = Density of fluid

#### **Abbreviation**

C.H.F = Constant Heat Flux  
 C.W.T = Constant Wall Temperature

### **References**

- [1] Schlichting, H., "Boundary-Layer Theory", McGraw-Hill Book Company, New York, Sixth edition, 1968.
- [2] Moller, M.Y. "Forced Convection Heat Transfer in Straight Tubes", M.Sc. thesis, Mechanical Engineering Department, University of Cranfield, 1968.
- [3] Al-Ali, H.H. "Simultaneously Developing Laminar Flow and Heat Transfer in the Entrance Region of Flat and Circular Conduits" Ph.D thesis, Colorado School of Mines, Golden, CO (USA), Jan., 1988.
- [4] Shirly, C.C, Nascimento and Joao, N.N Quaresma" Generalized Integral Transform Solution For Hydrodynamically Developing Non-Newtonian Flow in Circular Tubes" J. of the Braz. Soc. Of Mech.Sci and Eng., 2006.
- [5] Hornbeck, R.W., "Numerical Marching Techniques for Fluid Flows with Heat Transfer", National Aeronautics and Space Administration, Washington, 1973.
- [6] Holman, J.P., "Heat Transfer", McGraw-Hill Book Company, New York, sixth edition, 2000.